PASJ: Publ. Astron. Soc. Japan , 1–??,

ASCA Identification of SMC X-2 with the 2.37-s Pulsar Discovered by RXTE

Jun YOKOGAWA[1], Ken'ichi TORII[2], Takayoshi KOHMURA[3], and Katsuji KOYAMA[1,4]
[1]*Department of Physics, Graduate School of Science, Kyoto University, Sakyo-ku, Kyoto 606-8502*
jun@cr.scphys.kyoto-u.ac.jp
koyama@cr.scphys.kyoto-u.ac.jp
[2]*National Space Development Agency of Japan, 2-1-1 Sengen, Tsukuba, Ibaraki 305-8505*
torii.kenichi@nasda.go.jp
[3]*Department of Earth and Space Science, Graduate School of Science, Osaka University,*
1-1 Machikaneyama-cho, Toyonaka, Osaka 560-0043
tkohmura@ess.sci.osaka-u.ac.jp
[4]*CREST, Japan Science and Technology Corporation (JST), 4-1-8 Honmachi, Kawaguchi, Saitama 332-0012*

(Received 2000 November 20; accepted 2001 February 2)

Abstract

ASCA observed a new X-ray pulsar recently discovered with RXTE in the Small Magellanic Cloud, and detected coherent pulsations with a barycentric period of 2.37230 ± 0.00004 s. The position is determined within a $\sim 30''$ radius error, which is much more accurate than that reported with RXTE. Since the position error well overlaps to a $\sim 20''$ radius error of the SAS-3 transient source SMC X-2, and since the probability that an unrelated source falls in the error region by chance is estimated to be less than 0.1%, we conclude that SMC X-2 is the 2.37-s pulsar. The X-ray spectrum in the 0.7–10.0 keV band can be fitted with a model of a power-law continuum plus a fluorescent line from neutral or low-ionization iron. The pulse profile has a single peak below a few keV and gradually changes to be a double-peaked structure as the energy increases; in particular, the iron line band (6.0–7.0 keV) marginally shows a double-peaked profile similar to that of the higher energy band observed with RXTE.

Key words: pulsars: individual (SMC X-2) — stars: emission-line, Be — stars: neutron — X-rays: stars

1. Introduction

SMC X-2 was discovered with the SAS-3 satellite in 1977 (Clark et al. 1978), which was one of the three brightest X-ray sources in the Small Magellanic Cloud (SMC) at that time. The luminosity in the 2–11 keV band was 8.4×10^{37} erg s^{-1} (distance of 65 kpc is assumed throughout this paper), but one month later, the X-ray flux was found to be below the detection limit, hence the flux decreased by a factor of $\gtrsim 10$ (Clark et al. 1979). Although it was detected with the HEAO1 A-2 experiment in 1977 (Marshall et al. 1979), the Einstein IPC observation made in 1979 found no flux (Seward, Mitchell 1981). A ROSAT observation made in 1991 (Kahabka, Pietsch 1996) found a bright X-ray source, RX J0054.5−7340, with a luminosity of 2.7×10^{37} erg s^{-1} (0.15–2.4 keV) in the error region of SMC X-2. After half a year, this source was below the ROSAT detection limit; the luminosity was reduced by a factor of $> 6 \times 10^3$ (Kahabka, Pietsch 1996). An optical counterpart was first proposed by Pesch et al. (1977) and was resolved into two stars separated by $\sim 1''$ (Murdin et al. 1979). Murdin et al. proposed that the fainter object ("star 5B"), a B1e star with a V magnitude of 16.0, would be the counterpart of SMC X-2. The optical counterpart and the time variability in X-rays support that SMC X-2 is a Be/X-ray binary.

Recently, RXTE/ASM (All-Sky Monitor) detected a large outburst in the direction of SMC X-2 in 2000 January–April, with a maximum luminosity of $\sim 10^{38}$ erg s^{-1} at a distance of 65 kpc (Corbet et al. 2001). Corbet et al. also discovered coherent pulsations with a period of ~ 2.37 s in RXTE/PCA (Proportional Counter Array) observations. SMC X-2 is located near to the edge of the error circle of an $\sim 3'$ radius.

ASCA observed a region near SMC X-2 twice, before and after the outburst covered by the RXTE observations. In the latter observation, we found X-rays near the position of SMC X-2, thus confirming the 2.37-s pulsations (Torii et al. 2000), and determined the source position more accurately. In this paper, we report on these ASCA results and discuss the nature of this transient X-ray pulsar.

2. Observations and Data Reduction

The two ASCA observations were made on 1999 May 11–12 and 2000 April 25–26, or on 51309.584–51310.682 (hereafter, obs. 1) and 51659.507–51660.586 (obs. 2) in units of Modified Julian Day (MJD).

ASCA carries four XRTs (X-ray Telescopes, Serlemitsos et al. 1995) with two GISs (Gas Imaging Spectrometers, Ohashi et al. 1996) and two SISs (Solid-state Imaging

Spectrometers, Burke et al. 1994) on the focal planes. Since SMC X-2 was outside of the field of view (FOV) of the SIS in both observations, we do not refer to the SIS in this paper.

The GIS was operated in the normal PH mode with a time resolution of 0.0625/0.5 s for the high/medium bit rate. We rejected the GIS data obtained in the South Atlantic Anomaly, in low cut-off rigidity regions (< 4 GV), or when the target's elevation angle was low ($< 5°$). Particle events were removed by a rise-time discrimination method. After screening, the total available exposure times of obs. 1 and 2 were ~ 41 ks and ~ 26 ks, respectively. To increase the statistics, we combined the data from GIS-2 and GIS-3 in following analyses.

We also refer to the data of ROSAT/PSPC and SAX/MECS observations made on 1991 October 9–November 2 and 1998 July 24, or on 48538.129–48562.471 and 51018.104–51018.623 (MJD). We retrieved the screened data sets with exposure times of ~ 1.3 ks and ~ 29.9 ks, respectively, from the HEASARC Online Service.

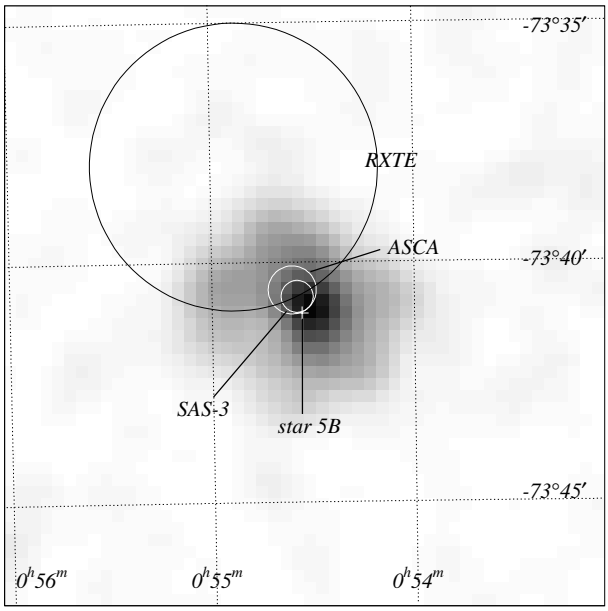

Fig. 1. ROSAT PSPC image near RX J0054.5−7340. The error circles of SAS-3, ASCA, and RXTE are given by the solid lines. The plus sign indicates the position of the proposed optical counterpart, "star 5B."

3. Results

3.1. Source Identification

No X-rays were detected near the position of SMC X-2 in the first ASCA observation (obs. 1), with a 2-σ upper limit of $\sim 6 \times 10^{-4}$ count s^{-1} in the 2.0–10.0 keV band. In the second observation (obs. 2), however, we found an X-ray source near SMC X-2. The source position was determined by a method described by Gotthelf et al. (2000) to be $(\mathrm{R.A., Dec.})_{\mathrm{J2000}} = (00^{\mathrm{h}}54^{\mathrm{m}}36^{\mathrm{s}}.5, -73°40'35'')$, with an error radius of $\sim 30''$ at 90% confidence level.

For source identification, we made a ROSAT PSPC image during an outburst of RX J0054.5−7340, and plotted the error circles of SMC X-2 (SAS-3), the 2.37-s pulsar (RXTE), and the ASCA new source together with the position of the optical counterpart, as shown in figure 1. We found that the position determined with ASCA is consistent with those of SAS-3, ROSAT, and RXTE. The optical counterpart for SMC X-2 is located at the edge of the error circle of SAS-3, and is slightly out of the ASCA error circle.

3.2. Timing Analyses

For timing analyses, we extracted ~ 1300 photons, including ~ 260 background events, in the 1.0–10.0 keV band from a $3'$ radius circle around the source (in obs. 2). We corrected the photon arrival times to those at the barycenter. We then performed an FFT (Fast Fourier Transform) analysis, and detected a significant power at an ~ 2.37 s period. With an epoch folding search, we determined the pulse period more precisely to be 2.37230 ± 0.00004 s. Other than coherent pulsations, no aperiodic variability was found.

Figure 2 shows the pulse profiles in the energy bands of 0.7–2.0 keV, 2.0–6.0 keV, 6.0–7.0 keV, and 7.0–10.0 keV. The pulse profile shows a single broad peak at lower energies, while it becomes more complex as the energy increases. A double-peaked structure, also found in a RXTE observation, is seen in the 6.0–7.0 keV band and possibly in the 7.0–10.0 keV band, although the statistics are not good in these energy bands.

We also searched for coherent pulsations from the ROSAT/PSPC data. From a source circle of $4'$ radius, we extracted 356 photons including ~ 30 background events in the 0.6–2.0 keV band. After a barycentric arrival time correction for these photons, we performed an FFT and epoch folding search, but no significant pulsation was found. The upper limit of the pulsed fraction was estimated to be $\sim 60\%$ according to a method of Leahy et al. (1983).

3.3. Spectral Analyses

The spectrum was made using the photons in the same circle used in the timing analyses, while the background spectrum was taken from a source-free region near the source.

The background-subtracted spectrum is given in figure 3. We fitted the spectrum with an absorbed power-law model. Although this model was found to be statistically acceptable with a photon index of $\Gamma \sim 0.6$, a systematic data excess was found at around 6–7 keV. We therefore added a narrow Gaussian line to the model and fitted the spectrum again, causing the excess to disappear. Adding the two new parameters (E_{Gauss} and I_{Gauss}) for the line feature improved the χ^2 value by 7.3, which corresponds to a significance level of 97% in the F-test. The best-fit model and parameters are given in figure 3 and table 1, respectively. The line energy of 6.3 keV with 90% error range of 6.1–6.5 keV is consistent with the K-shell emission from neutral or low-ionization iron.

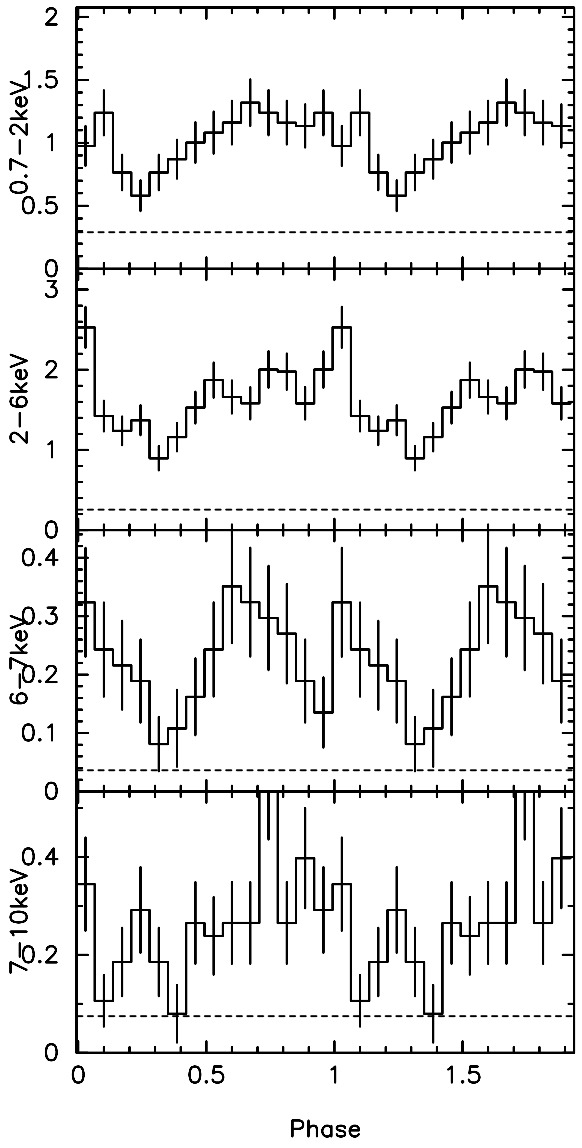

Fig. 2. Pulse profiles in the four energy bands, 0.7–2.0 keV, 2.0–6.0 keV, 6.0–7.0 keV, and 7.0–10.0 keV (from top to bottom). The vertical axes indicate the count rates multiplied by 100 in each energy band. The background levels are indicated by the broken lines. On- and off-pulse spectra were extracted from phases 0–0.15 plus 0.5–0.85 and 0.15–0.5 plus 0.85–1, respectively.

To examine the pulse phase dependence of the Gaussian component, we extracted phase-resolved spectra from phases 0–0.15 plus 0.5–0.85 ("on-pulse") and 0.15–0.5 plus 0.85–1 ("off-pulse"). "On-pulse" corresponds to the two bumps found in the pulse profile of the 6.0–7.0 keV band (see figure 2). We fitted these spectra to the same model, fixing the line energy ($E_{\rm Gauss}$) at 6.3 keV. The best-fit models and parameters are given in figure 4 and table 1, respectively. We found a hint of pulse phase variations in the line intensity and equivalent width (EW): larger values at on-pulse than those of off-pulse, although the limited statistics do not allow us to make any definite statements.

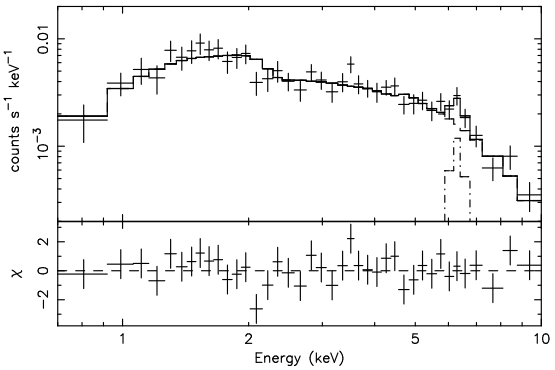

Fig. 3. Background-subtracted and phase-averaged spectrum obtained with GIS-2 + GIS-3. The crosses and the solid line indicate data points and the best-fit model, respectively. The dashed lines represent the power-law and the Gaussian components.

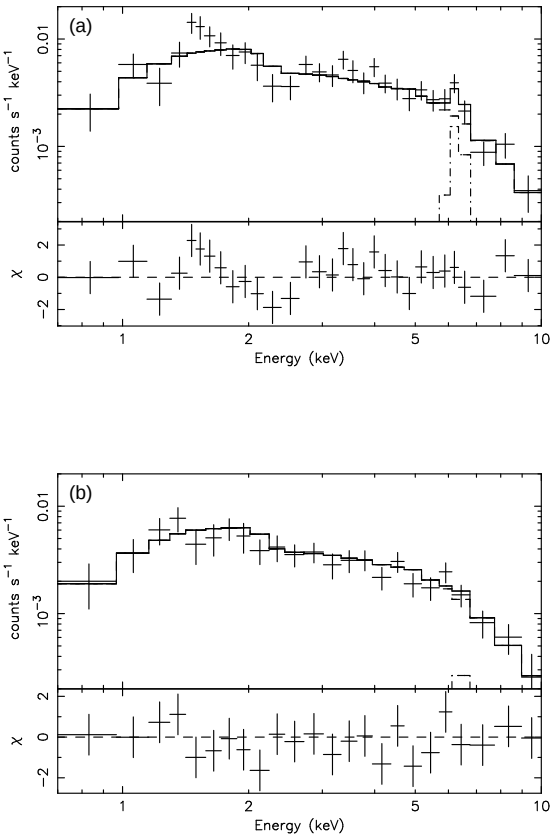

Fig. 4. Same as figure 3, but for phase-resolved spectra: (a) Pulse-on phase, (b) Pulse-off phase.

Table 1. Results of the spectral fitting.

Parameters	Phase-averaged	On-pulse	Off-pulse
Γ	0.7 (0.5–0.9)	0.7 (0.5–0.9)	0.7 (0.5–0.9)
$E^*_{\rm Gauss}$ (keV)	6.3 (6.1–6.5)	6.3 [fixed]	6.3 [fixed]
$I^*_{\rm Gauss}$ (10^{-5} photon s^{-1} cm^{-2})	4.4 (1.7–7.0)	6.4 (2.2–11)	2.1 (<5.5)
EW$^*_{\rm Gauss}$ (eV)	400 (150–640)	490 (170–840)	240 (<630)
$N_{\rm H}$ (cm^{-2})	0 ($<1\times10^{21}$)	0 ($<3\times10^{21}$)	0 ($<2\times10^{21}$)
Flux† (erg s^{-1} cm^{-2})	9.1×10^{-12}	9.9×10^{-12}	6.7×10^{-12}
Luminosity† (erg s^{-1})	3.9×10^{36}	4.3×10^{36}	2.9×10^{36}
χ^2/d.o.f.	31.08/34	31.43/26	10.76/19

Note — Parentheses indicate 90% confidence limits. Difference of d.o.f. between the on- and off-pulse spectra is due to the different number of bins in the spectra.

$*$: Central energy (E), intensity (I), and equivalent width (EW) of the Gaussian component.

†: Derived from the energy band of 2.0–10.0 keV. The distance is assumed to be 65 kpc.

3.4. Flux Upper Limits

We examined the flux history in the pre-outburst of this transient pulsar. Since we found no significant X-ray photons in the ASCA obs. 1 and the SAX observation, we derived the flux upper limit assuming the same spectrum in the outburst (obs. 2). The 2-σ flux/luminosity upper limits in these observations were estimated to be $\sim 3\times10^{-13}$ erg s^{-1} cm^{-2} or $\sim 1\times10^{35}$ erg s^{-1} (obs. 1) and $\sim 4\times10^{-13}$ erg s^{-1} cm^{-2} or $\sim 2\times10^{35}$ erg s^{-1} (SAX) in 2.0–10.0 keV, respectively.

4. Discussion

We found a transient pulsar with a period of 2.37230 ± 0.00004 s, which is in full agreement with the RXTE result (Corbet et al. 2001). The position error of $\sim30''$ radius is much smaller than that determined with RXTE. The positions of the transient sources found with SAS-3 (SMC X-2), ROSAT (RX J0054.5−7340) and RXTE/ASCA (the 2.37-s pulsar) overlap with each other within their relatively small errors of a few $\times\ 10''$ radius.

Only 8 sources brighter or equal to $\sim10^{38}$ erg s^{-1} have been found in the $\sim3^\circ\times3^\circ$ field of the SMC (SMC X-1, 2, 3, H0107−750, XTE J0111.2−7317, RX J0052.1−7319, RX J0059.2−7138, and RX J0117.6−7330: cf. Clark et al. 1978; Whitlock, Lochner 1994; Yokogawa et al. 2000; Kahabka 2000; Kohno et al. 2000; Macomb et al. 1999). The chance probability that two unrelated bright sources with a luminosity of $\sim10^{38}$ erg s^{-1} overlap within $\sim30''$ in the SMC is thus estimated to be less than 0.1%. We therefore conclude that SMC X-2, RX J0054.5−7340, and the 2.37-s pulsar are the same object observed in different transient episodes.

No detection of the 2.37-s pulsations from RX J0054.5−7340 would be due to the limited photon number; the pulsed fraction in the 0.7–2.0 keV band of ASCA was only $\sim60\%$, which is near the upper limit for the ROSAT source. The short pulse period of ~2 s, the existence of a Be star companion, and the highly transient nature of SMC X-2 are all similar to the properties of a pulsar RX J0059.2−7138 (Kohno et al. 2000; Hughes 1994), which is also located outside of the optical main body of the SMC.

We found an emission line at 6.3 ± 0.2 keV, which is attributable to a fluorescent line from neutral iron, or iron less ionized than Ne-like. This is the second detection of an iron line in the SMC pulsar, after XTE J0111.2−7317 (Yokogawa et al. 2000). Among 30–40 Be/X-ray binary pulsars (Be-XBPs) in our Galaxy (Liu et al. 2000), iron lines have been detected from only ~8 sources (4U 0115+63, 4U 1145−61, EXO 2030+375, 2S 0114+650, XTE J1858+034, XTE J1946+274, 1SAX J1452.8−5949, and GRO J1008−57: cf. Rose et al. 1979; Nagase et al. 1991; White et al. 1980; Parmar et al. 1989; Yamauchi et al. 1990; Oosterbroek et al. 1999; Shrader et al. 1999). Therefore, the detection of iron lines from Be-XBPs is rather rare even in our Galaxy. Since the metallicity of the SMC is only $\sim20\%$ of our Galaxy (Russell, Dopita 1992), the detection of iron lines from SMC X-2 with the EW of several hundred eV, which is among the largest in all the Be-XBPs, would be notable.

We are grateful to an anonymous referee for constructive comments and suggestions. We thank Dr. R.H.D. Corbet who gave us some results from RXTE observations of SMC X-2 before publication. J.Y. and T.K. are supported by JSPS Research Fellowship for Young Scientists. HEASARC Online System where we retrieved the ROSAT and SAX data is provided by NASA/GSFC.

References

Burke, B. E., Mountain, R. W., Daniels, P. J., Dolat, V. S., & Cooper, M. J. 1994, IEEE Trans. Nucl. Sci., 41, 375

Campana, S., Israel, G. L., Stella, L., & Santangelo, A. 1998, IAU Circ., 7039

Clark, G., Doxsey, R., Li, F., Jernigan, J. G., & van Paradijs, J. 1978, ApJ, 221, L37

Clark, G., Li, F., & van Paradijs, J. 1979, ApJ, 227, 54

Corbet, R. H. D., Marshall, F. E., Coe, M. J., Laycock, S., & Handler, G. 2001, ApJ, 548, L41

Gotthelf, E. V., Ueda, Y., Fujimoto, R., Kii, T., & Yamaoka, K. 2000, ApJ, 543, 417

Hughes, J. P. 1994, ApJ, 427, L25
Kahabka, P. 2000, A&A, 354, 999
Kahabka, P., & Pietsch, W. 1996, A&A, 312, 919
Kohno, M., Yokogawa, J., & Koyama, K. 2000, PASJ, 52, 299
Leahy, D. A., Darbro, W., Elsner, R. F., Weisskopf, M. C., Sutherland, P. G., Kahn, S., & Grindlay, J. E. 1983, ApJ, 266, 160
Liu, Q. Z., van Paradijs, J., & van den Heuvel, E. P. J. 2000, A&AS, 147, 25
Macomb, D. J., Finger, M. H., Harmon, B. A., Lamb, R. C., & Prince, T. A. 1999, ApJ, 518, L99
Marshall, F. E., Boldt, E. A., Holt, S. S., Mushotzky, R. F., Pravdo, S. H., Rothchild, R. E., & Serlemitsos, P. J. 1979, ApJS, 40, 657
McCray, R. A., Shull, J. M., Boynton, P. E., Deeter, J. E., Holt, S. S., & White, N. E. 1982, ApJ, 262, 301
Murdin, P., Morton, D. C., & Thomas, R. M. 1979, MNRAS, 186, 43
Nagase, F. 1989, PASJ, 41, 1
Nagase, F., Dotani, T., Tanaka, Y., Makishima, K., Mihara, T., Sakao, T., Tsunemi, H., Kitamoto, S., et al. 1991, ApJ, 375, L49
Ohashi, T., Ebisawa, K., Fukazawa, Y., Hiyoshi, K., Horii, M., Ikebe, Y., Ikeda, H., Inoue, H. et al. 1996, PASJ, 48, 157
Oosterbroek, T., Orlandini, M., Parmar, A. N., Angelini, L., Israel, G. L., Dal Fiume, D., Mereghetti, S., Santangelo, A., & Cusumano, G. 1999, A&A, 351, L33
Parmar, A. N., White, N. E., Stella, L., Izzo, C., & Ferri, P. 1989, ApJ, 338, 359
Paul, B., & Rao, A. R. 1998, A&A, 337, 815
Pesch, P., Sanduleak, N., & Philip, A. G. D. 1977, IAU Circ., 3127
Rose, L. A., Pravdo, S. H., Kaluzienski, L. J., Marshall, F. E., Holt, S. S., Boldt, E. A., Rothschild, R. E., & Serlemitsos, P. J. 1979, ApJ, 231, 919
Russell, S. C., & Dopita, M. A. 1992, ApJ, 384, 508
Serlemitsos, P. J., Jalota, L., Soong, Y., Kunieda, H., Tawara, Y., Tsusaka, Y., Suzuki, H., Sakima, Y. et al. 1995, PASJ, 47, 105
Seward, F. D., & Mitchell, M. 1981, ApJ, 243, 736
Shrader, C. R., Sutaria, F. K., Singh, K. P., & Macomb, D. J. 1999, ApJ, 512, 920
Torii, K., Kohmura, T., Yokogawa, J., & Koyama, K. 2000, IAU Circ., 7441
White, N. E., Pravdo, S. H., Becker, R. H., Boldt, E. A., Holt, S. S., & Serlemitsos, P. J. 1980, ApJ, 239, 655
White, N. E., Swank, J. H., & Holt, S. S. 1983, ApJ, 270, 711
Whitlock, L., & Lochner, J. C. 1994, ApJ, 437, 841
Yamauchi, S., Asaoka, I., Kawada, M., Koyama, K., & Tawara, Y. 1990, PASJ, 42, L53
Yokogawa, J., Paul, B., Ozaki, M., Nagase, F., Chakrabarty, D., & Takeshima, T. 2000, ApJ, 539, 191